

# Plasma Thruster Plume Simulation: Effect of Vacuum Chamber Environment

Passaro A.\*

*Aerospace Division – CPR, Ospedaletto, Pisa, 56121, Italy*

Vicini A.<sup>†</sup> and Biagioni L.<sup>‡</sup>

*Alta S.p.A. – via Gherardesca 5 – Pisa, 56121, Italy*

Present simulation techniques for plasma thrusters plume simulations usually implement a Particle In Cell / Monte Carlo approach to a plasma flow considered in a quasi-neutral state, with the possibility of a residual atmosphere (typical of a vacuum chamber test facility). Nonetheless it is difficult to compare directly results, even with measurements taken in very similar laboratory configurations, because it's not yet achieved the possibility to simulate at the same time realistic chamber geometry, pumping system performance and effect of the sputtering caused by the ion beam impinging the chamber walls. The present article will show the results of a series of PIC/DSMC simulations executed with CPR/Alta codes on HET plumes, considering a wide range of realistic laboratory configurations, and considering also the effect of different physical models; results will be also compared with experimental ones from literature and Alta testing facilities and flight data from the European SMART-1 mission.

## Nomenclature

$k$	= Boltzmann constant
$m_T$	= propellant mass-flow rate
$n$	= number density
$q$	= electron charge
$R$	= gas constant
$S$	= cryo-pumping surface
$T$	= temperature
$\dot{V}$	= pumping speed
$\epsilon$	= dielectric constant
$\phi$	= electrostatic potential
$\rho$	= charge density

## I. Introduction

Electric propulsion represents one of the most promising technologies for application in future space missions. Among the proposed concepts, Hall Effect Thrusters (HET's) and Gridded Ion Engines (GIE) are particularly interesting, for their relatively high thrust capability coupled with a specific impulse which is up to one order of magnitude higher than latest generation chemical systems.

The thruster plasma plume characteristics are defined by the combined effects of the dynamics of charged particles, which compose the relatively rarefied plume itself, and the magnetic field applied to the thruster. The knowledge of the plasma plume evolution in the thruster surrounding space is of fundamental importance, at system design level, for new generation satellites, in order to integrate the propulsive subsystem with the other vehicle subsystems: as known, the use of electro-magnetic thrusters can create compatibility problems, due to the

---

\* Graduate Student, [a.passaro@cpr.it](mailto:a.passaro@cpr.it), AIAA Student Member.

<sup>†</sup> Senior Scientist, Computational Engineering Dept., [a.vicini@alta-space.com](mailto:a.vicini@alta-space.com).

<sup>‡</sup> President & CEO, [l.biagioni@alta-space.com](mailto:l.biagioni@alta-space.com), AIAA Member.

electrically charged particle flow, which can interfere with telecommunication signals and generate erosion and insulation loss for critical satellite surfaces (e.g. solar panels, optical instruments and sensors etc.). Present simulation techniques usually implement a Particle In Cell / Monte Carlo approach to a plasma flow considered in a quasi-neutral state, with the possibility of a residual atmosphere (typical of a vacuum chamber test facility). Nonetheless it is difficult to compare directly results, even with measurements taken in very similar laboratory configurations, because it's not yet achieved the possibility to simulate at the same time realistic chamber geometry, pumping system performance and effect of the sputtering caused by the ion beam impinging the chamber walls.

During the last few years the numerical activities at Alta SpA and CPR, in Pisa, Italy, have been focused on plasma thruster plume simulation and interaction of plume with vacuum chamber environment: two *hybrid* PIC-MCC codes (one for axisymmetric simulation, one for 3D configurations) and a *neutral* DSMC code have been developed for simulations of realistic vacuum chamber geometries.

The present paper will illustrate the results obtained showing how the vacuum chamber system (geometry and pumping system) influences the thruster background and operation leading to significant differences between *on ground* and *in flight* plume behavior, although thruster data obtained from ground simulations can be successfully used for flight ones. In particular, results relative to the ESA's SMART-1 mission will be presented comparing simulation, ground, and flight data.

## II. Code description

Three codes were used for the activities summarized in this paper: two *hybrid* PIC codes and Bird's standard DSMC code. In the following sections a brief description of the two Alta's code will be presented, while information for Bird's code can be retrieved from Ref. 1.

### A. PICPluS 2

The PICPluS-2 code, developed at CPR-Alta, is meant to be a calculation and simulation instrument to study and predict the interaction between plasma thruster plumes and space vehicle surfaces. The plume characteristics are defined by the combined effects of charged particle dynamics, which compose the relatively rarefied plume itself, and the magnetic field applied to the thruster.

The present version of the code is a two-dimensional axially-symmetric *hybrid* PIC/MCC program<sup>5,7</sup>. Several different methods to characterize important features like electron temperature and collisions are implemented, in order to be able to assess possible effects of the simulation choices on the results. In particular, a fast SOR Poisson solver is included along with the possibility to use a quasi-neutrality approach to derive plasma potential. In the following sub-sections, a brief overview of the main code features is presented.

#### 1. Ions and neutrals

Several particle species can be independently simulated. Xenon propellant is currently used, but other propellants can be added. Background distributions of neutral propellant are included in the simulation. Neutral atoms, possibly exiting from the thruster due to the effective ionization rate, are also simulated (either through a MCC or DSMC approach<sup>1</sup>).

#### 2. Electrons

Electrons are assumed to form a collisionless, non magnetic, non isothermal fluid. The electron density is calculated by using the Boltzmann distribution (eq. 1), when needed modified in order to allow for the effect of non isothermal electron temperature  $T_e$ :

$$n_e(r, z) = n_{e\infty} e^{q\phi(r, z) / kT_e} \quad (1)$$

$$T_e(r, z) = \text{const} \quad (2a)$$

$n_{e\infty}$  is chosen in order to match electron temperature measurements. If the isothermal fluid approach is assumed electron temperature is considered constant (eq. 2a). If the non isothermal option is chosen, electron temperature can be retrieved from a simplified model using Chapman-Enskog approach<sup>1</sup> or by using the adiabatic approximation<sup>1,6</sup>. In the first case, considering Navier-Stokes-Fourier equations for electron fluid under stationary conditions and negligible electron drift velocity, only Laplace equation for  $T_e$  has to be solved. Retrieved electron temperature is held constant during the whole simulation allowing to compute it during the pre-processing phase.

If the adiabatic approximation is used, electrons are assumed to expand as a adiabatic fluid with temperature following eq. 2b:

$$T_e(r, z) = T_{ref} \left( \frac{n_e(r, z)}{n_{ref}} \right)^{\gamma-1} \quad (2b)$$

where  $\gamma = c_p/c_v$  is a number than can be set between 5/3 (monoatomic gas) and 1; in this case the electron temperature field is updated at each time step.

### 3. Potential and electric field

Electric potential can be retrieved, after coupling with the electron component, solving the non-linear Poisson equation

$$\nabla^2 \phi(r, z) + \frac{\rho_i(r, z)}{\epsilon_0} - \frac{\rho_{exc}}{\epsilon_0} e^{q\phi(r, z)/kT} = 0 \quad (3)$$

Equation 3 is linearized with a Newton-Raphson technique, while a relaxation technique is used to solve the linearized equation on the grid (finite differences). A Successive Over Relaxation (SOR) technique, based on checker-board ordering of updated cells is used and, in order to speed-up the relaxation, a Chebishev acceleration technique is implemented. Solution of the Poisson's equation was initially preferred to the hypothesis of plasma quasi-neutrality in the plume in order to investigate the validity of the quasi-neutrality assumption itself. After determination of potential, the electric field is calculated using alternatively a six-point Boris scheme for the gradient on the non-uniform grid or a typical two-point scheme. Alternatively, plasma quasi-neutrality can be imposed, deriving the electric potential from equation 1, once electron temperature and ion number density is known.

### 4. Collisions

Ion-neutral elastic and Charge Exchange (CEX) collisions can be included in the PIC cycle independently. Two different collisions models can be chosen; the first one is an implementation of the Variable Hard Sphere model, while the second is the induced dipole model of Nanbu<sup>10,3</sup>.

### 5. Grid and time-step

The considered physical domain is two-dimensional and axially symmetric, enclosed in a rectangular numerical domain in the  $(r, z)$  space. The grid is non uniform in both  $r$  and  $z$  coordinates in order to adapt to the local plasma density in a simple and straightforward way. For what concerns boundary conditions, the upper, right, and left boundaries are considered as outflow, while axial symmetrical boundary conditions are considered on the lower boundary. Some of the outer boundaries can be treated as solid walls at constant temperature and potential with ion impacts ranging between perfect reflection and full random diffusion, with partial thermal accommodation calculated using Cercignani-Lampis-Lord model<sup>1</sup>.

### 6. Injection data and applied magnetic field

Data regarding the particles distribution (number densities, velocities) at the exit of the thruster can be provided through an input file; alternatively, different internal models can be used to customize the distributions. For what concerns the magnetic field, the code is realized in order to work preferentially with experimental input data: an interpolation routine can be used to adjust any input data matrix on the computational grid. If data are not available, the required fields can be automatically generated by the code through various possible models or can be set at zero level.

## B. PICPluS3D

PICPluS3D is a 3D extension of the axial symmetric code described above: All the main features are maintained, the main simplification being the use of the quasi-neutrality hypothesis to compute plasma potential. This allows a considerable gain in computational efficiency; on the other hand, previous experience shows how the quasi-neutrality hypothesis doesn't have a significant impact for Hall thruster plasma flows, when compared to the full resolution of the Poisson equation<sup>3</sup>.

### III. Codes assessment

The plume simulation codes have been assessed using results of similar programs and available experimental data found in the literature, or produced in Alta's facilities. Figure 1 shows a comparison of experimental and computed (2D) current density for the 5 kW engineering HET model developed at Alta-CPR, and a quite good agreement can be observed (experimental current drop around  $-70^\circ$  is due to shadowing of the probe rake). Of course, as already mentioned by Van Gilder and Boyd<sup>12</sup>, the most important parameter determining plume behavior appears to be the inlet distributions used for ion injection. Several methods can be used considering both experimental distributions (when available) or mathematical ones. For what concerns Hall Effect Thrusters, "optimal" distributions can generally be found, allowing to fit satisfactorily near field and far field measurements. Figure 2 shows the comparison of computed current densities with the experimental ones by King<sup>8</sup> for the SPT-100

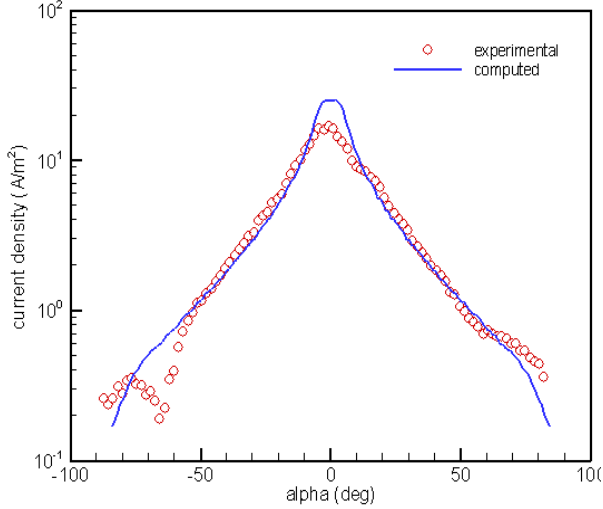


**Figure 1. Comparison of experimental and computed (2D) current densities at  $d=0.9$  m for the ALTA XH5 HET model.**

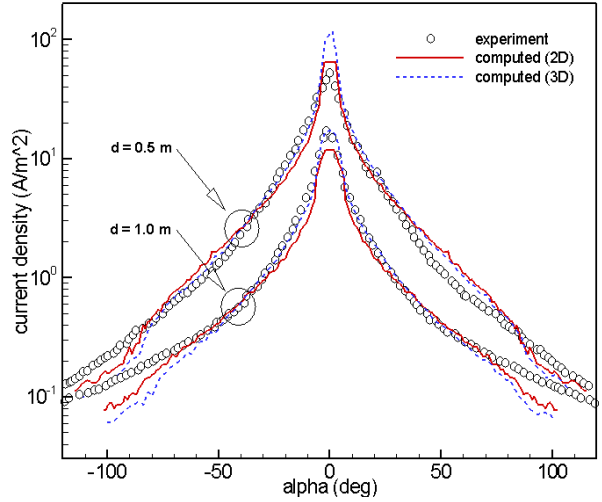


**Figure 2. Comparison of experimental and computed (2D & 3D) current densities for the SPT-100 thruster.**

thruster. For this distributions, ions are injected following a Gaussian pattern centered on the channel centerline while average divergence angle linearly increases from 0 deg on the centerline to 20 deg at the external radius but following a Gaussian distribution for each value of the average angle itself. In the figure the 2D and corresponding 3D simulations are illustrated, showing good agreement with experiment and good consistency between them.

### IV. Effects of vacuum facility on plume shape and thruster performances

Vacuum facilities for electric propulsion testing are usually vacuum vessels that operate, with thruster firing, at pressure levels of the order of  $10^{-4}$ - $10^{-6}$  mbar. Several different arrangement of pumps and, in particular, of cryogenic surfaces can be individuated for the same vacuum vessel with different results for what concerns its performance. In fact, while traditionally the nominal pumping speed can be retrieved from the hardware specification, and the pressure level of the chamber can be retrieved simply considering the thruster mass flow, it is worth<sup>1</sup> to introduce an *effective* pumping speed which is directly related to the background pressure *around* the thruster.

#### A. Vacuum facility and effective pumping speed

For a specified pumping surface, the nominal pumping speed can be computed by gas kinetic theory, assuming a unit sticking coefficient:

$$\dot{V}_p = S_p \sqrt{\frac{RT_b}{2\pi}} \quad (4)$$

where  $R$  is the gas constant ( $63.32 \text{ J kg}^{-1} \text{ K}^{-1}$  for Xenon),  $S_p$  is the panel surface and  $T_b$  is the prevailing background gas temperature; this method can only provide preliminary information about the facility performance, as it is not accounting for pumping speed losses caused by pressure gradients established within the vacuum vessel. In fact, in situations like the one depicted in Fig. 3, in which the gas load and the pumping actions are applied in substantially separated regions of the vacuum enclosure, relatively large dynamic pressure gradients can establish within the tank and, in the region where the thruster is located, a larger than expected number density may be present. Propulsive tests (and especially EPS tests) present some singular features, which are separating them from other space simulation experiments. In fact, in the latter case the gas load is usually in the form of thermalised gas molecules, with a velocity distribution which is essentially Maxwellian in magnitude and random in direction. On the other hand, in EPS tests the gas load is in the form of a highly directional, non-thermal ion beam, which enters the vacuum vessel on one side and crosses (in a mostly non-collisional way) the tank before thermalising on the opposite wall (beam target). It is convenient, when dealing with EPS (or more in general propulsion system) tests, to define an “effective pumping speed” based on the vacuum level that is established (in dynamic conditions) in close proximity of the operating thruster:

$$\dot{V}_{p,eff} = \frac{m_T R}{n_{b,T} k} \quad (5)$$

where  $m_T$  is the thruster mass flow rate,  $n_{b,T}$  is the background number density in the thruster region and  $k$  is the Boltzmann constant ( $1.38 \cdot 10^{-23} \text{ J K}^{-1}$ ). In general terms, the effective pumping speed is a function of the geometry and temperature distribution on the facility walls and pumping plates, and of the thruster plume characteristics: the effective pumping speed as computed using the equation above may be smaller, equal or larger than the nominal pumping speed, and is essentially a figure of merit of the overall facility performance for a specific thruster.

### B. Effects on background pressure and plume shape

The pressure inside the chamber is affected only in a limited way by the thruster’s plume: a background pressure of  $10^{-5}$  mbar at room temperature, corresponds to a Xenon number density of about  $2.4 \cdot 10^{17} \text{ m}^{-3}$  while typical plasma thruster exhausts have comparable number density for a distance in the order of 0.5 m around the thruster itself. As shown also by Walker *et al.*<sup>13</sup>, the pressure value equalizes around the background value very close to the thruster. At the same time, the presence of a so high neutral density increases dramatically the number of collisions for plume ions spreading significantly the plume: a typical increase of 10 deg can be observed for the plume divergence half-angle in ground experiment compared to the expected values from theory or simulations. Finally, gradients in the background pressure typically due to the individual chamber arrangement (see. Fig. 4), and that usually *are not* included in simulations, complicate furthermore the situation.

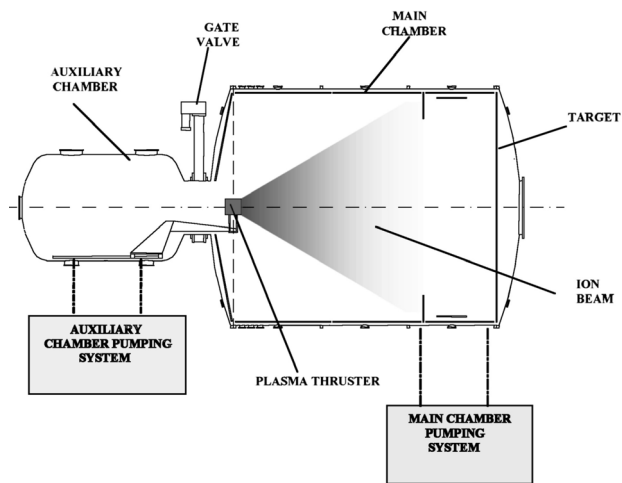


Figure 3. Overall facility layout for Alta Large Space Simulator, including a Main Chamber (6 m diameter) and an Auxiliary Chamber (2 m diameter) connected by a large gate valve.

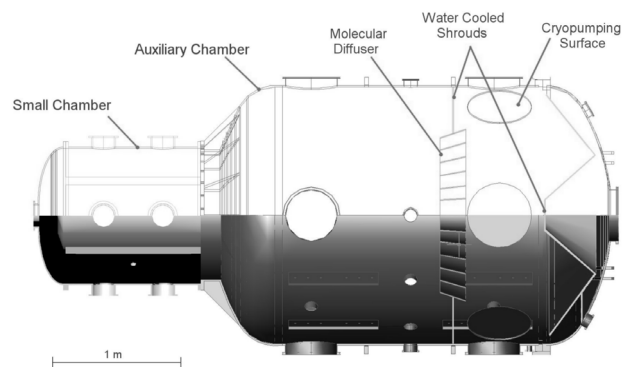
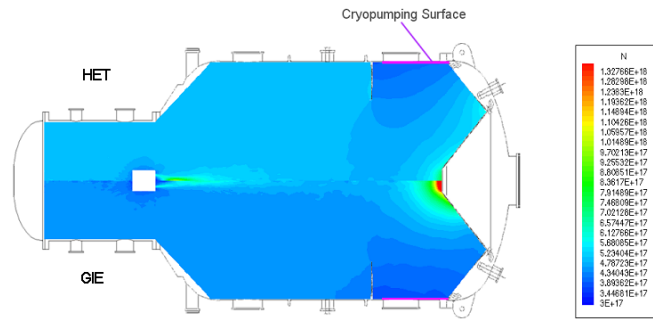


Figure 4. Chamber arrangement for Alta IV-4 facility: cryo-panels separated via water-cooled shrouds from plume volume and possibility of use of a molecular diffuser.



load from the tank walls: this load is the maximum that can be removed by the cold heads operating at less than 50 K. At the prevailing background temperature inside the main tank, the 1.1 m<sup>2</sup> cryopumping surfaces are nominally rated to about 64,000 l/s [Xe]. A set of DSMC simulations was used in order to define the most efficient pumping configuration in order to maximize the effective pumping speed on Xenon (i.e. minimize background pressure closer to thruster) with results showing how, with proper target and cold-head configuration an increase of effective pumping speed up by about 15% was possible. Simulations were confirmed by experiments with different thruster running continuously in the chamber with different mass flow rates: pressure was acquired in 4 points located along the chamber axis showing that, in the region close to the thruster, measured pressure was within 1% of the simulated value.



**Figure 6. DSMC results for IV-4 facility (number density).**

### B. Thruster performance and plume shape: comparison with ground and flight data (PIC-MCC)

Results will here be presented pertinent to the PPS-1350 thruster installed on the SMART-1 satellite. The nominal characteristics of the thruster are summarized in Table 1.

Propellant flow rate (anode)	4.21 10 <sup>-6</sup> kg/s
Discharge voltage	350 V
Discharge current	3.47 A
Thrust	72.1 mN

**Table 1. PPS-1350 working parameters.**

An assessment of the plume simulation has been carried out using the corresponding experimental data; for this case, a current density rake measured at a distance of 0.65 m from the thruster in a vacuum chamber facility was available, together with RPA measurements of the LABEN EPDP<sup>9</sup> device in flight conditions. The experimental current density was used in a preliminary investigation with the purpose to devise the ions ejection conditions from the thruster that best fit the experimental distribution. To this purpose, the ions distributions at the exit of the acceleration channel are represented using Gaussian distributions for both number density and velocity angle. This investigation was carried out using the axysymmetric version of the PICPluS code, with a background pressure  $p = 1 \cdot 10^{-2}$  Pa. Figure 7 shows the comparison between the experimental and the computed current density: on the left the results obtained using ions starting conditions similar to those characteristic of an SPT-100 thruster are illustrated; on the right, the results obtained with the final “optimum” ions starting conditions can be seen. It is apparent that a probe bias also need to be simulated. These conditions were subsequently used for a 3D plume simulation in flight conditions. The geometry model used for the satellite is illustrated in Fig. 8, together with a sketch of the computational grid; it includes the satellite main body and part of the solar cells panels, and the extension of the simulation domain is 2 m in every direction from the thruster. The computed current density is shown in Fig. 9, compared with the experimental one and that obtained through 2D simulations in vacuum chamber conditions. It can be seen that in flight conditions the whole plume shape is changed, also at low angles; the plume is more focused, and this also results in a higher computed thrust (about 10%).

The EPDP RPA instrument is located on the same face of the satellite of the thruster, at a distance of 0.47 m from the latter, and of about 0.05 m from the satellite face. Figure 10 shows the comparison between charge exchange ions energies obtained from the RPA measurements and the corresponding computation obtained using a virtual instrument. It can be seen how the agreement is quite good for the primary

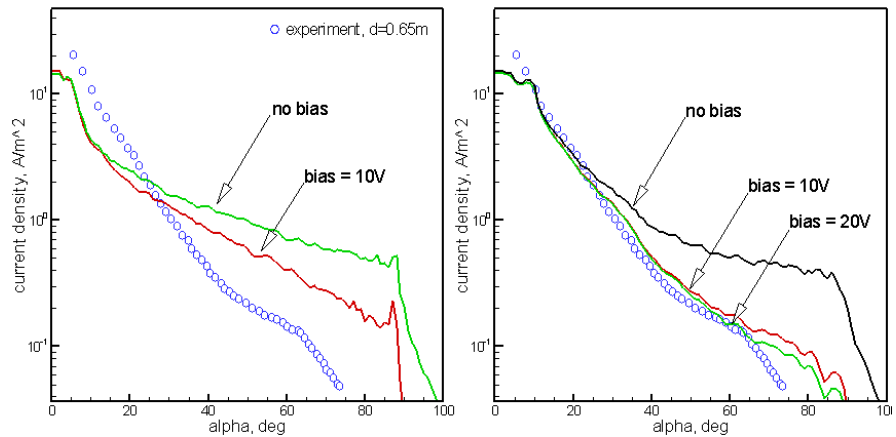


Figure 7. Computed current density distributions for the PPS-1350 thruster; initial (left) and final (right) ions ejection conditions.

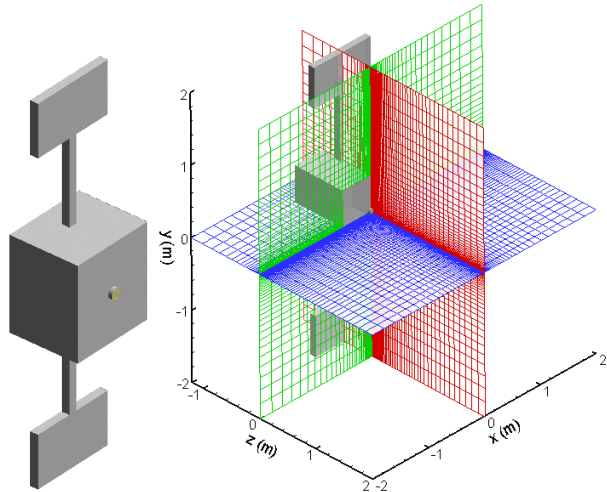


Figure 8. Sketch of the geometry model and of the computational grid used for the SMART-1 test case.

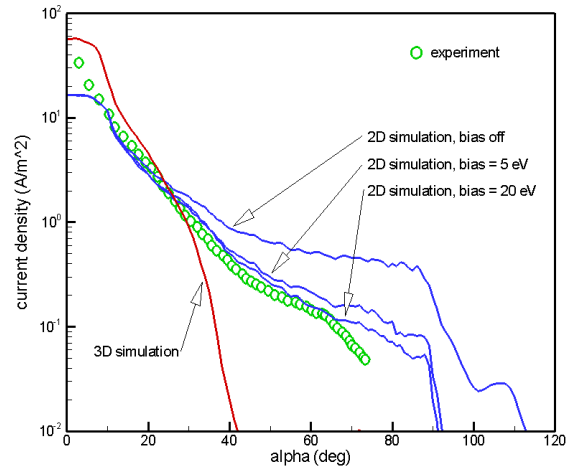


Figure 9. Comparison of the current density computed in vacuum chamber and in flight conditions.

energy peak, and also the secondary peak, which is due to the presence of double charged ions in the simulation, is well represented. The magnitude of this secondary peak is dependent on the percentage of double charged ions, that was here arbitrarily set to 25%. The high energy tail shown by the measurement is missing in the computation; this could be possibly obtained by using a longer sampling time for the virtual probe, as “events” up to energies of 100 eV are recorded in the simulation. It must be noted that the RPA data have been shifted to the left of 18V: the shift can be possibly due to the instrument floating potential, but investigations on this topic are still underway.

In Fig.11 the ions energy distributions computed by three virtual probes in flight conditions (vacuum) and in a vacuum chamber environment ( $p=10^{-2}$  Pa) are illustrated. The first probe is at the EPDP instrument position, the second at a point  $30^\circ$  off the axis, and the third on the axis; in all cases, the distance from the thruster is 0.47 m. It can be seen how the distributions at the points inside the main beam is similar; in the vacuum chamber ions are slightly more energetic at the probe #2 position, and

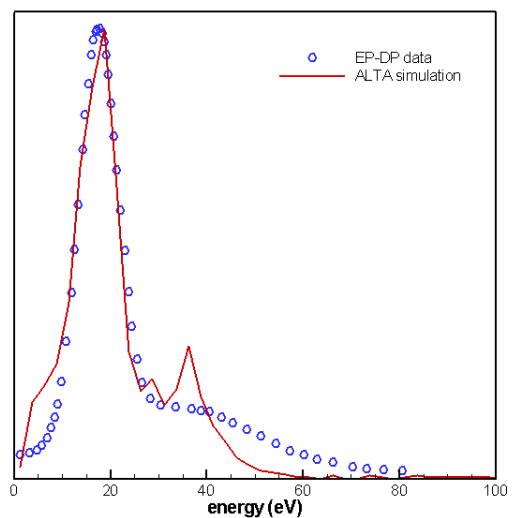
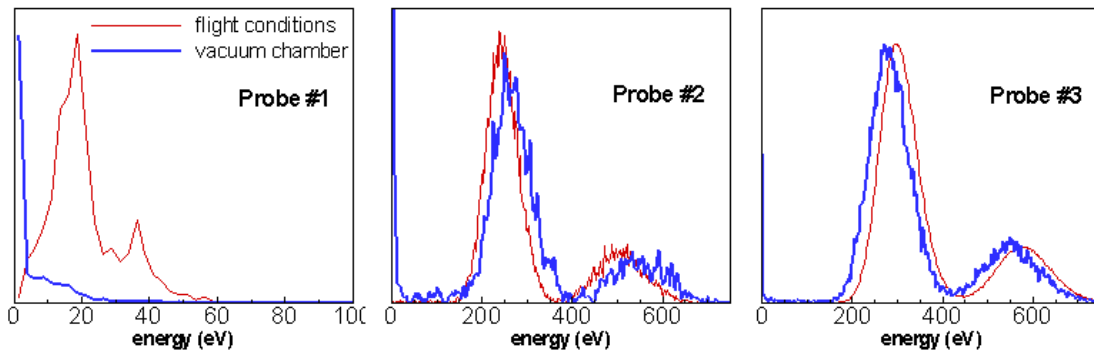


Figure 10. Comparison between in flight RPA data and simulation

slightly less on the axis; in both cases in the experimental facility conditions the presence of ions with energy less than 20 eV is also recorded. The situation is instead quite different for probe #1; in this case, with the high



**Figure 11. Comparison between ions energy distributions computed in flight and vacuum chamber conditions. Probe #1: EPDP position; probe #2: 30° off axis; probe #3: on thruster axis.**

background pressure only energies lower than 30 eV may be observed.

### C. Erosion and sputtering (PIC-MCC and DSMC)

The SMART-1 in HBF3 for the End to End EP Test, was simulated considering different possible geometries for the beam target that had to be placed close to the thruster due to the peculiar chamber geometry. A preliminary set of simulations using only Xenon particles to simulate the thruster plume was carried out in order to identify effective pumping speed and plume behavior. A successive set of multi-species DSMC simulations was therefore performed with graphite or steel macro-particles emitted by the surfaces hit by the plasma plume. Evolution of the sputtered particles was followed along the chamber and a qualitative index of deposition was individuated for the satellite surfaces. Pressure measurements carried out during the test were within 2% from computed values.

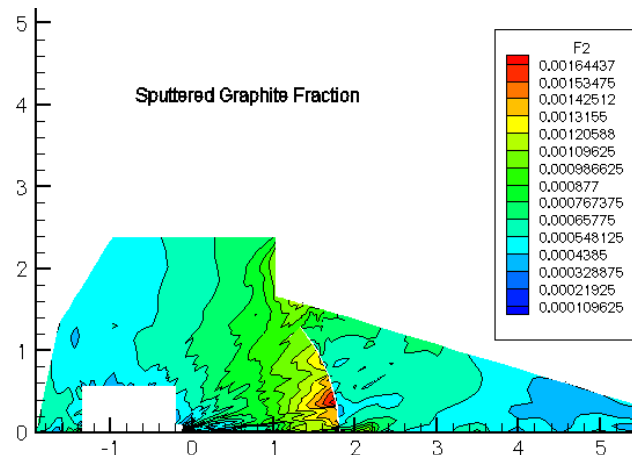


**Figure 12. DSMC results for sputtered graphite fraction within ESA's HBF3 facility for the SMART-1 End to End EP Test.**

### D. Effect on numerical results (PIC-MCC)

Plume shape is heavily influenced not only by the background pressure, but also by vacuum chamber solid walls (and other possible features of the chamber). Ion trajectories and energy in fact vary considerably if the presence of the solid walls is simulated or not. This can be observed in Fig.13, showing ions number density distributions and trajectories obtained in the vacuum chamber, simulating or not the presence of the walls. A value of 0 has here been imposed

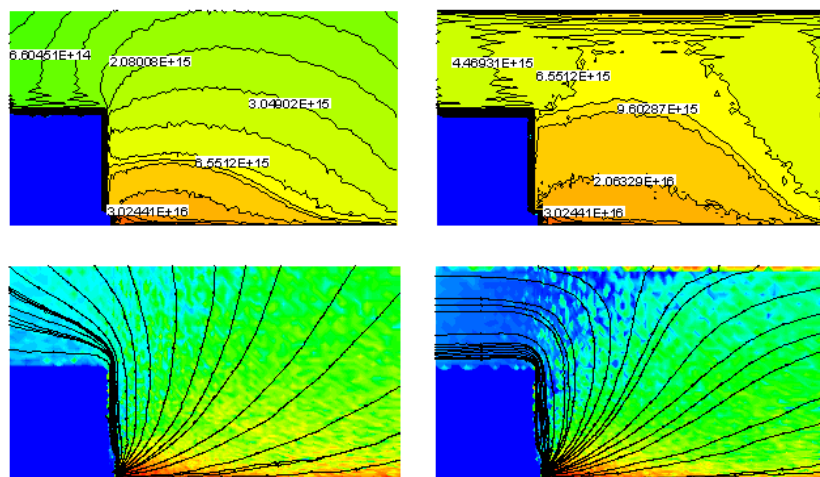


**Figure 13. Ions number density (above) and streamlines (below) computed in a vacuum chamber environment. On the left results obtained for an unconstrained flow; on the right the presence of the chamber walls is simulated.**

for the potential at the walls (grounding of chamber walls), and the ions impacting the wall are neutralized. Ion current density does not change much, though, due to the fact that the vast majority of ions are very slow CEX.

## VI. Conclusions

Plasma thrusters represent an extremely interesting technology for future space applications, but still need, at the present state knowledge, a great effort on ground characterization within proper vacuum chamber based facilities. The effects of the vacuum chamber environments are significant on a wide range of physical phenomena, directly interacting with the in-flight performances of the thruster and the possibility of extrapolating ground measurements to flight conditions. At the same time, vacuum chamber environment poses several issues with regard to the numerical reconstruction of the experiments that have to be taken in account in order to obtain significant results. CPR and Alta SpA dedicated during the last few years consistent efforts in order to individuate and develop a series of simulation instruments that can be used for design or diagnostic purposes. The paper showed how, applying different codes and different techniques to several practical cases, results that are within a few percentage points from measurements can be obtained. At the same time, it was possible to devise how, even if the chamber environment has such a big effect on the experiments, if a careful calibration process is conducted to tune the simulation code with the ground recorded data, significant results are obtained also for what concerns in-flight performance. RPA measurements taken by the Laben EPDP instruments on the ESA's SMART-1 satellite were satisfactorily reconstructed by the PICPLUS 3D code.

## Acknowledgments

The authors of this work have been actively supported for DSMC simulations by Mr. Claudio Reconditi whose help is gratefully acknowledged.

The authors also wish to acknowledge the help provided by Dr. David Nicolini of ESA-ESTEC concerning the SMART-1 HBF3 End to End EP Test, Mr. Jose Gonzalez del Amo and Mr. Eric Gengembre of ESA-ESTEC and Laben-PROEL for the SMART-1 in-flight data.

## References

1. Andrenucci, M., Biagioni, L., Passaro, A., *PIC/DSMC Models for Hall Effect Thruster Plumes: Present Status and Ways Forward*, AIAA Paper 2002-4254, July 2002.
2. Biagioni, L., Passaro, A., Andrenucci, M., *Particle Simulation of Tailored Vacuum Pumping Configurations for Electric Propulsion Testing*, presented at the 4<sup>th</sup> International Symposium on Environmental Testing for Space Programmes Liege, June 2001.
3. Biagioni, L., Passaro, A., Vicini, A., *Plasma Thruster Plume Simulation: Effect of the Plasma Quasi Neutrality Hypothesis*, 34th AIAA Plasmadynamics and Lasers Conference, Orlando FL, 23-26 June 2003.
4. Bird, G.A., *Molecular Gas Dynamics and the Direct Simulation of Gas Flows*, Oxford Science Publications, Oxford, 1994.
5. Birdsall, C.K., Langdon, A.B., *Plasma Physics Via Computer Simulation*, McGraw-Hill, New York, 1985.
6. Celik, M., Santi, M., Cheng, S., Martinez-Sanchez, M., Peraire, J., *Hybrid-PIC Simulation of a Hall Thruster Plume on an Unstructured Grid with DSMC Collisions*, presented at the 28<sup>th</sup> IEPC, Toulouse, March 2003.
7. Hockney, R.W., Eastwood, J.W., *Computer Simulation Using Particles*, McGraw-Hill, New York, 1981.
8. King, L.B., *Transport Property and Mass Spectral Measurements in the Plasma Exhaust Plume of a Hall Effect Space Propulsion System*, Ph.D. Dissertation, Dept. Of Aerospace engineering, Univ. Of Michigan, Ann Arbor, MI, May 1998.
9. Matticari, G., Noci, G., Estublier, D., Gonzales del Amo, J., Marini, A., Tajmar, M., *The Smart-1 Electric Propulsion Diagnostic Package*, proceedings of the 3rd Spacecraft Propulsion Conference, 2000.
10. Nanbu, K., (2000), *Probability Theory of Electron-Molecule, Ion-Molecule, Molecule-Molecule, and Coulomb Collisions for Particle Modeling of Materials Processing Plasmas and Gases*, IEEE Transactions on Plasma Science, Vol.28, No.3.
11. Taccogna, F., Longo, S., Capitelli, M., *Particle-in-Cell with Monte Carlo Simulation of SPT-100 Exhaust Plumes*, J. of Spacecraft and Rockets, Vol.39, No.3, May-June 2002.
12. Van Gilder, D.B., Boyd, I.D., *Particle Simulations of the SPT-100 Plume*, AIAA Paper 98-3797, 1998.
13. Walker, M. L. R., Gallimore, A. D., Cai, C., Boyd, I. D., *Pressure Map of a Facility as a Function of Flow Rate to Study Facility Effects*, AIAA paper 2002-3815, 38th Joint Propulsion Conference, Indianapolis, IN, July 7-10, 2002.